The Brewster effect in exciton reflectance spectra

A. B. Pevtsov and A. V. Sel'kin

A. F. Ioffe Physicotechnical Institute, Academy of Sciences of the USSR, Leningrad

(Submitted 29 January 1982)
Zh. Eksp. Teor. Fiz. **83**, 516–531 (August 1982)

The conditions under which the Brewster effect manifests itself in exciton oblique-reflectance spectra are considered for the first time. It is shown that, in the isolated-exciton-resonance model that takes account of the spatial dispersion and the presence on the crystal surface of an exciton-free homogeneous dielectric layer, the reflectance can vanish completely for either the *p*- or *s*-polarized component within the limits of the exciton reflectance band. The amplitude-phase spectral dependence of the reflectance has been experimentally investigated for the crystals ZnTe, ZnP_2 ($T = 2$ K), and CdS ($T = 2$ and 77 K) in the case of oblique incidence of the light in the region of the lowest exciton resonances. The results show that the exciton Brewster effect occurs in all these crystals (in the case of ZnP_2 it manifests itself in the *s*-polarized component). The theoretical model satisfactorily describes the experimental data.

PACS numbers: 78.20.Dj, 71.35. + z

INTRODUCTION

It is well known that there can be found in the case of oblique incidence of light at the plane boundary of a transparent dielectric medium an angle of incidence $\varphi = \varphi_{BR}$, called the Brewster angle, at which the energy reflectance R_p measured in the *p*-polarized component vanishes (see §1.5 of Ref. 1 and §4.2 of Ref. 2). The φ dependence of the phase difference $\Delta = \Delta_p - \Delta_s$ between the *p*- and *s*-polarized components of the reflected wave then undergoes at the point φ_{BR} a jump equal to $\pm\pi$.

The occurrence of absorption in the medium leads to an increase in the coefficient R_p ($R_p \neq 0$) at the angle φ_{BR} and the "smearing" of the sharp jump in the function $\Delta(\varphi)$. In such cases we can speak of the Brewster angle only conditionally, taking φ_{BR} to be the "pseudo-Brewster" (Ref. 2, §4.2) angle of incidence at which the reflectance assumes its minimum value as φ is varied. But if the surface of the absorbing substrate-medium is covered with a transparent dielectric film, then there can be established conditions under which the exact Brewster effect occurs,[1)] i.e., under which $R_p = 0$ (Ref. 1, §13.5). Moreover, the reflectance R_s for the *s*-polarized component can also vanish when certain relations connecting the parameters of the film and those of the substrate are fulfilled.[3]

In view of the foregoing, it is of interest to study the Brewster effect in the oblique-incidence reflectance spectra in the region of the exciton resonances of semiconductor crystals, for which the role of a transparent film can be played by an exciton-free surface layer,[4] the so-called "dead" layer (DL). There then arise new possibilities of experimental and theoretical investigation of the surface region of a crystal, spatial dispersion (SD), polaritonic effects, and other exciton-related optical properties of a semiconductor.[5,6] The problem of choosing the boundary conditions correctly acquires especial importance.[6]

In the present paper we show that the Brewster effect can be observed in its full sense in light scattering in the strong-exciton-absorption-band region as well. In this case the conditions for the occurence of the effect are determined by both the volume parameters of the exciton resonance and the properties of the surface transition region.

The paper consists of two chapters. Chapter I is theoretical. In it we expound the theory of the Brewster effect in the isolated-exciton-resonance model with allowance for the SD and the DL (§1). For the purpose of simplifying the analysis of the effect, in §2 of Chap. I we derive simple approximate relations connecting the parameters of the theory, and constituting the conditions under which the Brewster effect is possible. In §3 we perform on the basis of the exact formulas numerical computations demonstrating the conditions for the occurrence of the effect, and discuss the results of this numerical analysis on the basis obtained in §2.

Chapter II is devoted to the experimental investigation of the Brewster effect in the region of the exciton resonances. In §1 of this chapter we describe the procedural features of the experiment. In §2 we present the main results of the investigation of the exciton Brewster effect in the reflectance amplitude and phase spectra of the crystals ZnTe, ZnP_2, and CdS. A comparison of the results of the theoretical calculation with the experimental data is carried out in §3 of Chap. II.

I. THEORY

§1. The Brewster effect in the "dead" layer model

The question of the role of the surface and SD in the shaping of the optical spectra of crystals in the exciton-resonance frequency region has been repeatedly considered in the literature.[6] Diverse sets of boundary conditions have been proposed for the description of the experimental data, and the particulars of the behavior of an exciton near the crystal boundary have been discussed. The DL model, which was proposed back in 1963 by Hopfield and Thomas,[4] occupies a special place among the existing models for the boundary conditions.

Later this model was generalzied to the case of oblique reflection, and has, on the whole, been successfully used to

 0038-5646/82/080282-09$04.00

analyze the exciton reflectance spectra of a number of crystals: GaAs,[7] ZnO,[8] InP,[9] CdS,[10-12] CuCl,[13] ZnSe,[14] AgI,[15] ZnTe,[16] and ZnP_2.[17] This circumstance apparently reflects a fairly general phenomenon characteristic of the most perfect crystals, and consisting in a relatively rapid increase of the potential energy of a mechanical exciton as it approaches the crystal surface within a distance l of the order of the exciton radius.

We shall perform the analysis of the Brewster effect in the exciton region of the spectrum within the framework of a theory that takes account of the SD, assuming the existence at the crystal boundary of a dead (exciton-free) layer, on the inner surface of which Pekar's additional boundary conditions[5] are valid. Let us consider the neighborhood of a dipole-active exciton resonance, whose permittivity can be represented in the form[6]

$$\varepsilon(\omega,\mathbf{K})=\varepsilon_0\left(1+\frac{\omega_{LT}}{\omega_0-\omega+\hbar K^2/2M-i\Gamma/2}\right), \tag{1}$$

where ω_0 is the resonance frequency of the exciton, M is its translational mass, Γ is the damping constant, ω_{LT} is the longitudinal-transverse splitting, and ε_0 is the background permittivity. The dependence of $\varepsilon(\omega,\mathbf{K})$ on the wave vector $\mathbf{K}$ arises when the mass M is finite, and corresponds to the consideration of the SD.[5,6]

The formula (1) can be expressed either as the scalar permittivity in a cubic crystal, or as some permittivity-tensor element corresponding to the light polarization for which a dipole transition into a lower-symmetry exciton crystal state is allowed. The DL is usually specified by its thickness l and the permittivity ε_0, which coincides with background value of $\varepsilon(\omega,\mathbf{K})$.

The system under consideration is essentially an absorbing crystal-susbtrate whose surface is covered with a transparent dielectric film. Therefore, it is convenient to represent the amplitude reflectance r in the form[1]

$$r=(r_0+r_1e^{2i\theta})/(1+r_0r_1e^{2i\theta}), \tag{2}$$

where r_0 is the amplitude reflectance for light incident from vacuum at some angle φ to the normal to the surface of a semi-infinite medium with permittivity ε_0, r_1 is the amplitude reflectance for light incident at an angle of $\varphi_1 = \arcsin(\sin\varphi/\sqrt{\varepsilon_0})$ from a medium with permittivity $\varepsilon(\omega,\mathbf{K})$, and

$$\theta=(\omega/c)\,l(\varepsilon_0-\sin^2\varphi)^{1/2}$$

is the phase thickness (the advance of the light-wave phase in a single transmission through the layer).

The formula (2) is valid for an angle φ of incidence for both the p- and the s-polarized components, including the possibility of allowing for the SD in the coefficient r_1. The value of r_0 is computed from the standard Fresnel formula, while for the computation of r_1 we must use the SD theory. The procedure for computing r_1 is well known,[10] and therefore we shall not dwell on it here.

From the formula (2) we obtain the "Brewster condition" ($r=0$)

$$i\,\mathrm{tg}\,\theta=(r_0+r_1)/(r_0-r_1), \tag{3}$$

which can be regarded as a system of two nonlinear equations for the quantities ω and Γ. The solutions, ω_{BR} and Γ_{BR}, to this system depend on the values of the angle φ of incidence and the parameters of the exciton resonance. The angle φ at which the condition (3) is realized has the meaning of the Brewster angle φ_{BR}.

§2. Approximation of normal incidence at the layer-crystal boundary

In the general case Eq. (3) is solved numerically with a computer. But using reasonable assumptions about the parameters of the problem, we can represent the relation (3) in a form that is convenient for analysis. In fact, we can usually assume that

$$\sin^2\varphi\ll\varepsilon_0,\quad q_0^2\equiv\hbar\omega_0^2\varepsilon_0/2Mc^2\lesssim\omega_{LT}. \tag{4}$$

For example, for CdS in the region of the $A_{n=1}$ exciton resonance,[12] we have $\varepsilon_0=10$, $\hbar q_0^2=7\times10^{-2}$ meV, $\hbar\omega_{LT}=2$ meV.

By neglecting in the r_1 calculation the corrections of the order of $\sin^2\varphi/\varepsilon_0$ in comparison with unity, we can show that r_1 does not depend on φ, i.e., that $r_1(\varphi)\approx r_1(0°)$. Then the right-hand relation in (4) gives the condition under which the contribution of the longitudinal exciton to the amplitude of the reflected wave can be neglected, and from the relation (3) we obtain in explicit form dependences that correspond to the condition $r=0$ of the frequency ω and the damping constant Γ on θ and φ:

$$\omega_{BR}+i\Gamma_{BR}/2=\omega_L+[q_0-q_\alpha(\varphi_{BR})\,\Phi_\alpha(\theta,\varphi_{BR})]^2,\quad \alpha=1,2,3. \tag{5}$$

Here $\omega_L=\omega_0+\omega_{LT}$ is the longitudinal frequency of the exciton; the values of the subscript $\alpha=1,2$ pertain to the case of the p component of the reflection, with $\alpha=1$ if $\varepsilon_0\cos^2\varphi_{BR}>1$ and $\alpha=2$ if $\varepsilon_0\cos^2\varphi_{BR}<1$; the value $\alpha=3$ pertains to the case of the s component:

$$q_1=q_2=(\omega_{LT}/|\varepsilon_0\cos^2\varphi_{BR}-1|)^{1/2},\quad q_3=[\omega_{LT}/(\varepsilon_0-1)]^{1/2};$$
$$\Phi_1=|\cos\theta|+i\varepsilon_0^{1/2}|\sin\theta|\cos\varphi_{BR},$$
$$\pi k\leqslant\theta\leqslant\arccos(q_0/q_1)+\pi k, \tag{6}$$
$$\varepsilon_0^{-1/2}\leqslant\cos\varphi_{BR}\leqslant[(1+\omega_{LT}/q_0^2)/\varepsilon_0]^{1/2},$$
$$\Phi_2=i\Phi_1^*,$$
$$\pi(k+1/2)\leqslant\theta\leqslant-\arcsin[q_0/(q_2\varepsilon_0^{1/2}\cos\varphi_{BR})]+\pi(k+1), \tag{7}$$
$$[(1+\omega_{LT}/q_0^2)/\varepsilon_0]^{-1/2}\leqslant\cos\varphi_{BR}\leqslant\varepsilon_0^{-1},$$
$$\Phi_3=|\cos\theta|\cos\varphi_{BR}+i\varepsilon_0^{1/2}|\sin\theta|,$$
$$\pi k\leqslant\theta\leqslant\arccos[q_0/q_3\cos\varphi_{BR}]+\pi k,\quad q_0/q_3\leqslant\cos\varphi_{BR}\leqslant1. \tag{8}$$

The inequalities (6), (7), and (8), which determine the regions of allowed values of θ and φ_{BR}, follow from the condition $\Gamma_{BR}\geqslant0$. The index k assumes integral values: $k=0,1,\ldots$.

The formula (5) is a simple analytic relation connecting the crystal parameters in the exciton-resonance region and the frequency and damping-constant values, ω_{BR} and Γ_{BR}, at which the Brewster effect is possible. The computational error given by the left inequality in (4) is, as a rule, within the limits of the errors in the experimental determination of the

parameters of the exciton resonance. Therefore, the relations obtained by us can in practice be used in the analysis of the experimental data.

A number of interesting circumstances following from the above-obtained formulas are noteworthy.

1. First of all it can be seen that, depending on the specific values of the parameters, the Brewster angle φ_{BR} in the exciton-resonance region can vary within wide limits (see (6)–(8)) including the value $\varphi_{BR} = 0°$.

2. The possibility of the occurrence of the Brewster effect is also determined by specific parameters. There exist parameter values at which the effect is not realized at all. In particular, the presence of SD ($q_0 \neq 0$) limits the range of allowed values of φ and l.

3. As can be seen from (5) and (8), the reflectance can also vanish in the case of the s-polarized component.

4. The frequency ω_{BR} and the damping constant Γ_{BR} are periodic functions (with period π) of the phase thickness θ. This fact also follows directly from the formula (2).

5. The φ_{BR} dependences of ω_{BR} and Γ_{BR} for the p-polarized component have poles at the point $\varphi_{BR} = \arccos(\varepsilon_0^{-1/2})$. The meaning of these poles is that they correspond in the approximation (4) to the "background" Brewster angle $\varphi_0 = \arctan(\varepsilon_0^{1/2})$.

6. The expression (5) is exact in the case when $\varphi_{BR} = 0°$. Then $q_1 = q_3$ and $\Phi_1 = \Phi_3$, which corresponds to the physical indistinguishability of the s- and p-polarized components in the case of normal incidence of the light.

Let us analyze the $\varphi_{BR} = 0°$ case in greater detail, since the reflectance spectra are most often investigated for angles of incidence close to normal incidence. Separating the real and imaginary parts in the expression (5), we can easily show that, for $\varphi_{BR} = 0°$,

$$\omega_{BR} = \omega_L + (q_3|\cos\theta| - q_0)^2 - \varepsilon_0 q_3^2 \sin^2\theta,$$
$$\Gamma_{BR} = 4\varepsilon_0^{1/2} q_3 |\sin\theta| (q_3|\cos\theta| - q_0), \tag{9}$$

where the range of allowed θ values is determined by the inequalities (6) or (8) with $\varphi_{BR} = 0°$ and $q_0/q_3 \leqslant 1$.

In the absence of SD (i.e., for $q_0 = 0$) the latter relation is clearly fulfilled; in this case (see (8)) the quantity θ can assume values from the region $\pi k \leqslant \theta \leqslant \pi(k + \frac{1}{2})$ ($k = 0,1,...$), and the Brewster effect in the case of normal incidence of the light is impossible in the interval $\pi(k + \frac{1}{2}) < \theta < \pi(k + 1)$. As the SD parameter ($q_0$) increases, the range of allowed values of θ (and, hence, l) shrinks, and when $q_0 > q_3$ the reflectance does not vanish at any value of the layer thickness l.

§3. The conditions for the occurrence of the Brewster effect: The results of the numerical analysis

Figure 1 shows the ω_{BR} and Γ_{BR} dependences of the DL thickness l, as computed for $\varphi_{BR} = 0°$ from the formulas (9). The computations were carried out for several values of the mass M (in units of the free-electron mass m_0) with ε_0-, ω_0-, and ω_{LT}-parameter values characteristic of the $n = 1$ exciton in ZnTe.[16] It can be seen that as M increases (i.e., as the contribution of the SD decreases), the area enclosed in Fig. 1a by the ordinate axis and the curve $l(\Gamma_{BR})$ increases, and is greatest at the maximum value of M. The range of allowed values of ω_{BR} (Fig. 1b) also broadens with increasing M in this case. The dashed horizontal straight line in the upper part of Fig. 1 indicates the DL-thickness value,

$$l_{\pi/2}^{(0)} = \pi c / 2\omega_0 \varepsilon_0^{1/2},$$

corresponding to a $\theta = \pi/2$ phase advance over this thickness in the case of normal incidence. The vertical arrows T and L in Fig. 1b indicate the positions of the transverse (ω_0) and longitudinal (ω_L) frequencies respectively.

The dependence $l(\Gamma_{BR})$ for the parameters of the $A_{n=1}$ exciton in CdS and for $\varphi = 0°$ was actually constructed by Komarov *et al.*[18] by computer calculation. But the fact that this curve gives a relation between l and Γ that corresponds to the condition $r = 0$ was not noticed. The conditions under which this curve exists were also not determined. The formulas (9) obtained by us not only allow us to analyze the qualitative characteristics of the functions $l(\Gamma_{BR})$ and $l(\omega_{BR})$, but also enable us to compute them easily and exactly.

We computed the curves $l(\Gamma_{BR})$ and $l(\omega_{BR})$ for the case of oblique incidence of the light by numerically solving Eq. (3) without the use of the approximations (4) with the aid of a computer. The results of the calculation performed for the Brewster effect in the p-polarized component with the characteristic parameters of ZnTe (Ref. 16) are shown in Fig. 2. It can be seen from this figure that indeed there exist for the p component in accordance with the formulas (5)–(7) two families of $l(\Gamma_{BR}, \omega_{BR})$ curves characterizing the Brewster condition in the exciton reflectance spectrum. One family is located in the region $0 \leqslant l \leqslant l_{\pi/2}^{(\varphi_0)}$, where

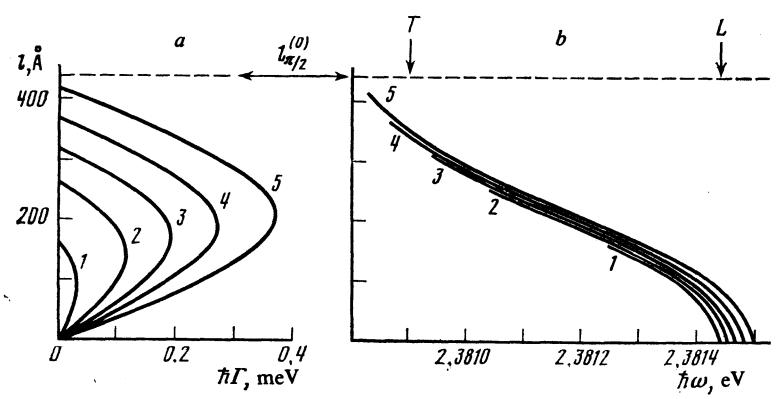

FIG. 1. Dependence of the dead-layer thickness l on (a) the damping constant $\Gamma = \Gamma_{BR}$ and (b) the frequency $\omega = \omega_{BR}$ at which the Brewster effect in the case of normal incidence of the light is possible. The curves were computed with the exciton-resonance parameters of ZnTe (see Table I) and different values of the translational exciton mass M: $M/m_0 = 1$ (the curve 1), 2 (2), 4 (3), 10 (4), and 100 (5), where m_0 is the free-electron mass.

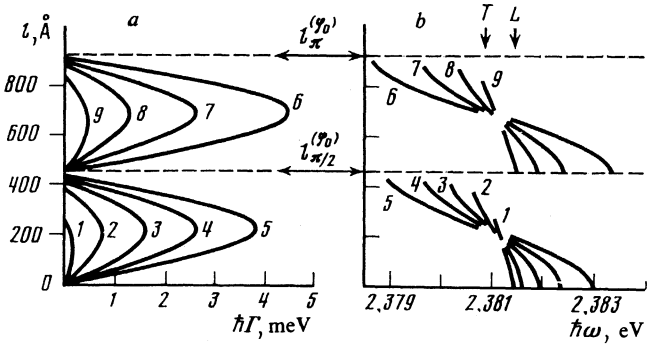

FIG. 2. Dependence of the dead-layer thickness l on (a) the damping constant $\Gamma = \Gamma_{BR}$ and (b) the frequency $\omega = \omega_{BR}$ at which the Brewster effect in the case of oblique incidence of the light is possible for the p-polarized component. The curves were computed with the exciton-resonance parameters of ZnTe (see Table I) and different values of the angle of incidence $\varphi = \varphi_{BR}$: $\varphi = 0°$ (the curve 1), 60° (2), 66° (3), 68° (4), 69° (5), 73° (6), 74° (7), 76° (8), and 80° (9).

$$l_{\pi/2}^{(\varphi_0)} = \pi c/2\omega_0(\varepsilon_0 - \sin^2\varphi_0)^{1/2}$$

is the layer thickness corresponding to a $\theta = \pi/2$ phase advance for a background Brewster angle equal to φ_0 (in this case $\varphi_{BR} < \varphi_0$). The other family of curves lies in the interval $l_{\pi/2}^{(\varphi_0)} \leqslant l \leqslant l_{\pi}^{(\varphi_0)}$, where $l_{\pi}^{(\varphi_0)} = 2l_{\pi/2}^{(\varphi_0)}$ corresponds to the value $\theta = \pi$ for $\varphi = \varphi_0$ (in this case $\varphi_{BR} > \varphi_0$). When $l \geqslant l_{\pi}^{(\varphi_0)}$, the curves $l(\Gamma_{BR})$ and $l(\omega_{BR})$ repeat with period $l_{\pi}^{(\varphi)}$ the dependences shown in Fig. 2.

As the angle φ_{BR} approaches the background value φ_0, the range of l values at which the Brewster condition can be realized broadens, which is a consequence of the SD. In the absence of SD, for any value of l, we can choose the remaining parameters such that the Brewster condition $r = 0$ is satisfied. The range of admissible values of the frequency ω_{BR} also broadens as φ_{BR} approaches φ_0. It can be seen from Fig. 2a that, if $\varphi_{BR} < \varphi_0$ ($l < l_{\pi/2}^{(\varphi_0)}$), then for a fixed layer thickness l the increase of Γ_{BR} leads to the increase of the angle φ_{BR}; when $\varphi_{BR} > \varphi_0$ ($l > l_{\pi/2}^{(\varphi_0)}$), the value of φ_{BR} decreases with increasing Γ_{BR}.

An interesting characteristic of the behavior of the $l(\omega_{BR})$ curves manifests itself in Fig. 2b; these curves are characterized by a narrow intersection region localized near the values $l = l_{\pi/2}^{(\varphi_0)}/2$ and $l = 3l_{\pi/2}^{(\varphi_0)}/2$ between the frequencies ω_0 and ω_L. Turning to the formulas (5)–(7), we see from them that, in the absence of SD, this region of intersection shrinks to the point with coordinates $\omega_{BR} = \omega_0 + \omega_{LT}/2$ and $l = l_{\pi/2}^{(0)}/2$ ($\varphi_{BR} < \varphi_0$) or $l = 3l_{\pi/2}^{(0)}/2$ ($\varphi_{BR} > \varphi_0$). The indicated values of the thickness correspond in the approximation (4) to a $\theta = \pi/4$ or $\theta = 3\pi/4$ phase shift in the layer. In the presence of SD such a point of intersection strictly does not exist. But because of the relative weakness of the SD, on the scale of Fig. 2b, the $l(\omega_{BR})$ curves practically intersect at one point.

Extremely interesting consequences follow from the possibility of the existence of the Brewster effect in the s-polarized component (see (5) and (8)). Figure 3 shows the dependences $l(\Gamma_{BR})$ (a) and $l(\omega_{BR})$ (b) for different values of the angle of incidence φ_{BR} for the case of the s component, as

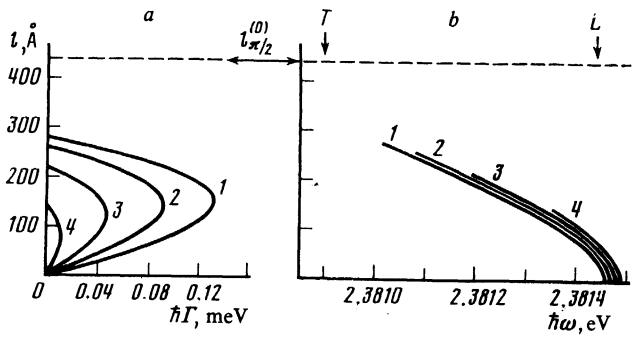

FIG. 3. Dependence of the dead-layer thickness l on (a) the damping constant $\Gamma = \Gamma_{BR}$ and (b) the frequency $\omega = \omega_{BR}$ at which the Brewster effect in the case of oblique incidence is possible for the s-polarized component of the light. The curves were computed with the exciton-resonance parameters for ZnTe (see Table I) and difference values of the angle of incidence $\varphi = \varphi_{BR}$: $\varphi = 0°$ (the curve 1), 30° (2), 45° (3), and 55° (4).

calculated with the aid of a computer with the parameters of ZnTe. These dependences constitute families of curves lying in the region $0 \leqslant l \leqslant l_{\pi/2}^{(0)}$, where $l_{\pi/2}^{(0)}$ is the layer thickness introduced earlier, and corresponding to a $\theta = \pi/2$ phase advance in the case of normal incidence of the light. When $l > l_{\pi}^{(0)} = 2l_{\pi/2}^{(0)}$, the curves $l(\Gamma_{BR})$ and $l(\omega_{BR})$ repeat with period $l_{\pi}^{(\varphi)}$ the dependences shown in Fig. 3. As the angle φ_{BR} increases, the range of l values at which the Brewster effect is possible in the s component shrinks, which is a consequence of the SD. In the presence of SD there exists some maximum value $\varphi_{max} \approx \arccos(q_0/q_3) < \pi/2$, of the angle of incidence, that limits the possibility of the observation of the effect to the region $0 \leqslant \varphi_{BR} \leqslant \varphi_{max}$. When $l_{\pi/2}^{(0)} < l < l_{\pi}^{(0)}$, the Brewster condition $r_s = 0$ is not realized at any values of the exciton-resonance parameters.

Comparing Figs. 2 and 3, we easily see that the Brewster condition (3) in the case of a cubic crystal cannot be simultaneously fulfilled for the s and p components under conditions of oblique incidence. Thus, if the Brewster effect is allowed in the s component, then it is forbidden in the p component, and vice versa.

For fixed layer parameters and a fixed angle of incidence, the frequency dependence of the energy reflectance $R = |r|^2$ is determined by the spectral behavior of the modulus $|r_1|$ and the phase Δ_1 of the coefficient $r_1 = |r_1|\exp(i\Delta_1)$, which characterizes the bulk properties of the crystal. Then, as was explained in §2, as the r_1 in the formula (2), we can approximately take its value for normal incidence. Figure 4 shows characteristic $|r_1|^2$ and Δ_1 spectra in the $\varphi = 0°$ case, constructed with the use of exciton-resonance parameters characteristic of ZnTe (Ref. 16) and two values of the damping constant: $\hbar\Gamma = 0.8$ meV (a, a') and $\hbar\Gamma = 0.01$ meV (b, b'). Notice that, on account of the adopted definition of the amplitude reflectances for the s-and p-polarized components, the phases of these reflectances differ by π in the case of normal incidence.[2] The phase curves a' and b' in Fig. 4 are for the case of p polarization.

II. EXPERIMENT

§1. Experimental procedure

The investigation of the exciton Brewster effect has to be performed under conditions of low reflectivity of the crys-

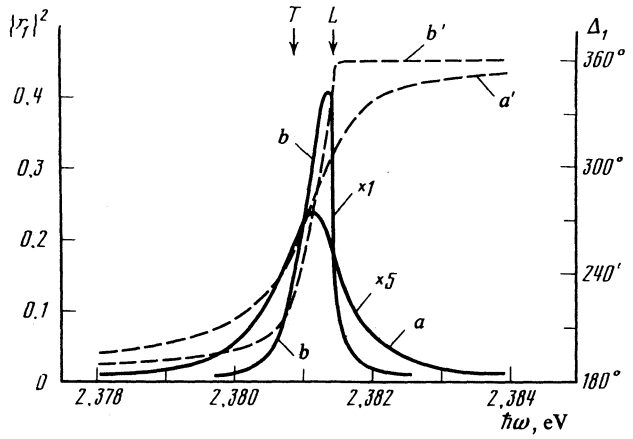

FIG. 4. Spectra of the reflectance $|r_1|^2$ (a, b) and the phase Δ_1 (a', b') of the coefficient r_1 in the case of normal incidence of the light from a medium of permittivity ε_0 (ε_0 is the background permittivity of the exciton resonance) on a crystal with permittivity $\varepsilon(\omega,\mathbf{K})$ that takes account of the resonance contribution of the exciton. The computations were performed with the parameters of ZnTe (see Table I) and two values of the damping constant Γ: $\hbar\Gamma = 0.8$ meV (a, a') and $\hbar\Gamma = 0.01$ meV (b, b').

tal. The measurements of the minimum values of the reflectance then entail difficulties connected with the presence of a diffuse component in the reflected light.[19] Therefore, to determine precisely when the Brewster effect occurs, it is not sufficient to determine the value of the angle of incidence φ at which the reflectance assumes its minimum value: it is also necessary to perform additional measurements of the phase of the reflected wave relative to the phase of the incident wave. The phase should undergo a jump equal to $\pm\pi$ at the point φ_{BR} when φ is varied.

It is possible to measure in the single-beam experimental scheme the phase difference $\Delta = \Delta_p - \Delta_s$ between the amplitude p and s components of the reflectance.[12,16,18,20,21] If one of the phases, Δ_p or Δ_s, undergoes a $\pm\pi$ jump, then their difference Δ should also undergo a corresponding jump.

In the experiment we measured the energy reflectance $R_\delta(\psi_0, \varphi, \psi)$ for different azimuths ψ_0 and ψ of the polarizer and analyzer and different angles of incidence. A phase plate allowing the establishment of an arbitrary additional phase shift δ between the p- and s-components of the reflected light was placed in the path of this light between the crystal and the analyzer. The azimuths ψ_0 and ψ were measured from the incidence plane clockwise when viewed in the direction of the wave vector of the light. The measurements were performed at crystal temperatures of 2 K (ZnTe, ZnP_2, CdS) and 77 K (CdS) on a setup based on a DFS-24 spectrometer. For the measurement at 77 K the crystal was directly immersed in liquid nitrogen, whose refractive index $n = 1.205$ (Ref. 22) was taken into account in the quantitative analysis of the spectra.

To find the quantity Δ, we used the relation[16]

$$\operatorname{tg}\Delta = [R_{-\pi/2}(45°, \varphi, 45°) - R_{-\pi/2}(45°, \varphi, 135°)]/$$
$$[R_0(45°, \varphi, 45°) - R_0(45°, \varphi, 135°)],$$

from which, knowing the signs of the numerator and the denominator, we can determine Δ to within an additive constant equal to $2\pi k$ ($k = 0, \pm 1, \ldots$). In this case the $R_\delta(\psi_0, \varphi, \psi)$ spectra were recorded in the photon-counting regime, which ensured a high signal-registration sensitivity in the region of minimum reflectivity, and at the same time preserved the maximum spectral resolution of the apparatus. The last two circumstances assured the necessary advantages of the procedure being described over the phase-measurement procedures used in the investigations reported in Refs. 12, 18, and 21.

The measurements of the coefficients $R_\delta(\psi_0, \varphi, \psi)$ were performed by us, using the method described in Ref. 11 (ZnTe, CdS), and with the aid of a standard mirror (ZnP_2). The divergence of the light beam was 3–4°. The geometry of the experiment and the procedure used in the present investigation are described in greater detail in our earlier publications.[12,16]

§2. The Brewster effect in the amplitude and phase spectra of the exciton reflectance of the crystals ZnTe, ZnP_2, and CdS

1. Cubic ZnTe crystals ($T = 2$ K)

The fact that the exact Brewster effect can be observed in the region of the strong exciton-absorption band was first noted in our previous paper,[16] where we reported an investigation of the amplitude-phase spectra of the reflectivity of ZnTe crystals, but did not carry out a detailed analysis of the effect. In the present paper, using the data obtained earlier,[16] we show how the exact Brewster effect can be experimentally identified.

The dots in Fig. 5 show the phase (i.e., Δ) spectra measured in the $n = 1$ exciton resonance spectral region of ZnTe crystals for angles of incidence $\varphi = 45°$ (1), 63° (3), and 82° (6). A comparison of the experimental curves 1 and 6 shows that

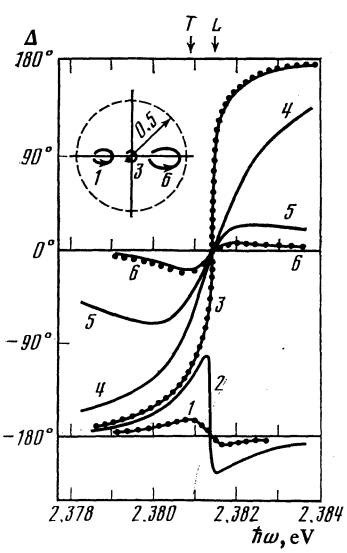

FIG. 5. Spectral dependence of the difference $\Delta = \Delta_p - \Delta_s$ between the phases of the reflectances r_p and r_s in the region of the lowest exciton state of ZnTe crystals ($T = 2$ K) for different angles of incidence of the light: $\varphi = 45°$ (the curve 1), 61° (2), 63° (3), 69° (4), 73° (5), and 82° (6). The points represent the experimental data; the curves, the theoretical results. The inset shows measured phase hodographs (plots of the quantity $\rho = |r_p/r_s|$ as a function of Δ in polar coordinates) for the angles of incidence $\varphi = 45°$ (1), 63° (2), 79° (3), and 82° (4).

the Δ spectrum for $\varphi = 82°$ is inverted with respect to the spectrum obtained at $\varphi = 45°$, and is shifted relative to it by π (along the Δ scale) at the ends of the spectral interval under consideration.

The character of the asymptotic behavior of the experimental curves 1 and 6 indicates that the Brewster angle, $\varphi_0^{(p)} = \arctan(\varepsilon_0^{1/2})$, corresponding to the background permittivity ε_0 at points far from resonance, lies in the range $45° < \varphi_0^{(p)} < 82°$. It is precisely at the value $\varphi = \varphi_0^{(p)}$ that the phase jump through π should occur when the frequency differs greatly from the resonance frequency ω_0. In order to ascertain how the transition from the curve 1 into the curve 6 occurs directly at resonance, we investigated the angular dependence of the Δ spectrum in the region $45° < \varphi < 82°$. It turned out that in the incidence-angle range $61° < \varphi < 71°$ the phase spectrum differs radically from the spectra 1 and 6: see the curve 3, which was measured at $\varphi = 63°$.

The transition of the phase spectrum from 1 through 3 into 6 is illustrated by the inset in the upper part of Fig. 5, which shows in polar coordinates the measured dependences of the quantity $\rho = (R_p/R_s)^{1/2}$ (R_p and R_s are the energy reflectances for the p and s components) on the phase angle Δ for $\varphi = 45°$ (1), 63° (3), and 82° (6). The angle Δ is measured counterclockwise from the horizontal axis (directed to the right). The radius of the dashed circle in the units in which ρ was measured is 0.5.

The $\rho(\Delta)$ dependences have the form of broken rings with the breaks corresponding to the ends of the spectral interval under consideration. The arrows on the rings indicate the direction of traversal into the region of higher frequencies. As the angle of incidence φ increases, these rings (phase hodographs) move from left to right. There comes a moment at some value of the angle φ when the phase hodograph crosses the coordinate origin. This means that the reflectance R_p vanishes, while the phase undergoes a $\pm\pi$ jump. Evidently, the angle at which the phase hodograph crosses the coordinate origin has the meaning of the Brewster angle $\varphi_{BR}^{(p)}$. The frequency $\omega_{BR}^{(p)}$ at which the effect is observed lies in the narrow region where the phase Δ assumes the value 0° (the curves 3 and 6) or $-180°$ (the curve 1).

At a higher value of φ the coordinate origin lies inside the hodograph ring, which corresponds to the case of a total phase change of 2π (the curve 3). The background Brewster effect is realized (in a frequency region far from resonance, where $\varphi \approx \varphi_0$) when the break in the hodograph is at the coordinate origin. In the case, investigated by us, of zinc telluride crystals $\varphi_{BR}^{(p)} = 62°$ and $\varphi_0^{(p)} = 71°$. And, finally, when $\varphi > \varphi_0^{(p)}$, the hodograph ring lies to the right of the coordinate origin (the curve 6), which corresponds to a spectral Δ function (the curve 6) that is inverted in shape with respect to the curve 1.

2. Orthorhombic ZnP_2 crystals ($T = 2$ K)

It has been shown[17] that some of the crystals of the black modification of ZnP_2 possess orthorhombic macrosymmetry, and have in the region 1.560–1.568 eV a very intense reflectance line corresponding to the dipole-active

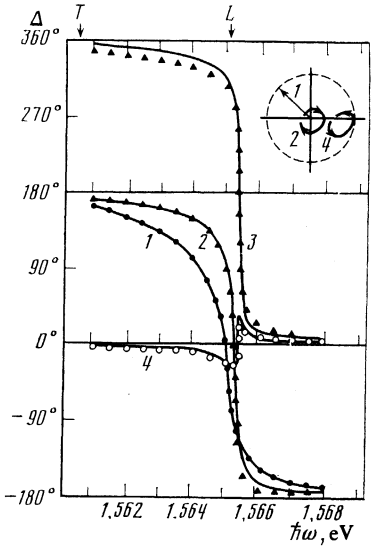

FIG. 6. Spectral dependence of the difference $\Delta = \Delta_p - \Delta_s$ between the phases of the reflectances r_p and r_s in the region of the lowest dipole-active exciton state of orthorhombic ZnP_2 crystals ($T = 2$ K) for different angles φ of incidence of the light: $\varphi = 10°$ (the curve 1), 65° (2), 79° (3), and 85° (4). The points represent the experimental data; the curves, the theoretical results. The inset shows measured phase hodographs (plots of the quantity $\rho = |r_p/r_s|$ as a function of Δ in polar coordinates) for angles of incidence $\varphi = 65°$ (2) and 85° (4). The crystal is oriented in such a way that the optical transition into the exciton state is allowed only for the s-polarized component of the light.

transition into the $n = 1$ exciton state. In this case an optical transition is allowed only for the polarization $\mathbf{E} \| C_{2z}$, where C_{2z} is one of the twofold axes. Using for the reflectivity investigation the crystal face parallel to the C_{2z} axis, and orienting this axis perpendicularly to the plane of incidence, we were able to study the exciton Brewster effect connected only with the s-polarized component. We did not find any exciton contribution to the p polarization of the reflected light.

Figure 6 shows the $\Delta = \Delta_p - \Delta_s$ phase spectra of orthorhombic zinc diphosphide for angles of incidence $\varphi = 10°$ (the closed circles on the curve 1), 65°, 79° (the triangles on the curves 2 and 3), and 85° (the open circles on the curve 4). A comparison of the curves 2, 3, and 4 shows that the important qualitative changes in the phase spectrum occur in the region of angles of incidence $65° < \varphi < 85°$. The fact that the curve 4 is shifted by $\sim\pi$ with respect to the curve 2 at the ends of the spectral interval in question indicates the existence of the normal (nonexciton) Brewster effect for the p-polarized component. On the other hand, the radical change that occurs in the shape of the phase spectrum on going from the curves 2 and 3 to the curve 4 is a consequence of the exciton Brewster effect.

Unfortunately, the limited incidence angle resolution does not allow a sufficiently graphic experimental demonstration of the detailed transition from the curve 3 to the curve 4. But using the values of the parameters of the $n = 1$ exciton resonance in ZnP_2, that were obtained by us as a result of the theoretical analysis of the reflectance amplitude-phase spectra, we determined the exciton Brewster angle $\varphi_{BR}^{(s)} = 81.9°$ for the s component and the normal Brewster angle $\varphi_0^{(p)} = 72.5°$ for the p component. Thus, as the

angle of incidence is increased, there occurs first the normal Brewster effect in the p component, which leads to a 180° shift (along the Δ scale) of a phase curve of the type 2 (see the curve 3 for $\varphi = 79°$). Then the exciton Brewster effect occurs, which implies a transition from the curve 3 to the curve 4.

The inset in Fig. 6 shows the experimentally measured phase hodographs corresponding to the spectral dependences 2 and 4. The arrows on the hodograph rings indicate the directions of increase of the frequency, and the breaks correspond to the ends of the spectral interval in question. The coordinate origin lies inside the ring 2; therefore, the total phase change is $\approx 2\pi$ (cf. the curve 2 of the spectral function $\Delta(\omega)$). The curve 4 does not enclose the coordinate origin; therefore, the phase returns to the initial value when the frequency passes through a resonance (cf. the curve 4 of the function $\Delta(\omega)$).

Notice that in the cases 1–3 the direction of circulation about the hodograph ring is clockwise. On the other hand, in the case 4 the direction of circulation is counterclockwise. Thus, the exciton Brewster effect in the s-polarized component is accompanied by a change in the direction of circulation about the phase-hodograph ring, which is a characteristic difference between this case and the case of the exciton Brewster effect in the p component (see Fig. 5). Furthermore, the phase-hodograph curve lies at infinity when the angle of incidence is exactly equal to $\varphi_{BR}^{(s)}$ at the frequency $\omega_{BR}^{(s)}$, which corresponds to the vanishing of the coefficient R_s in the ratio $\rho = (R_p/R_s)^{1/2}$.

3. Hexagonal CdS crystals ($T = 2$ and 77 K)

We investigated the reflectance amplitude-phase spectra of cadmium sulfide crystals in the $A_{n=1}$ exciton resonance spectral region. The hexagonal axis C_6 of the crystal lay in the plane of the reflecting crystal face, and was perpendicular to the plane of incidence. Since the transition into the $A_{n=1}$ state[4] is allowed in the dipole approximation only for the polarization $\mathbf{E} \perp C_6$, it was possible to investigate in the chosen reflection geometry the exciton Brewster effect connected only with the p-polarized component.

At a temperature $T = 2$–4.2 K, the phase Δ for CdS crystals in the case of normal incidence of the light changes by 2π within the limits of the $A_{n=1}$ exciton resonance region.[12,21] We investigated the dependence of the spectrum $\Delta(\omega)$ on the angle of incidence at 2 K. The experimental data are represented by the closed circles in Fig. 7 (the angles of incidence $\varphi = 45°$ (1) and 80° (2)). As the angle of incidence is increased, the measured phase hodograph (in the inset) moves from left to right, crossing the coordinate origin with its break when the angle of incidence is equal to the background Brewster angle $\varphi_0^{(p)} = 72.5°$. Thus, the variation of the shape of the phase curve (see the curves 1 and 2 and of the spectral function $\Delta(\omega)$ in Fig. 7) in the present case is connected with the background Brewster effect. The exciton involving the vanishing of the reflectance R_p does not occur.

At $T = 77$ K the CdS crystal, immersed directly in liquid nitrogen, has the phase spectra shown in Fig. 8 ($\varphi = 10°$ (1), 60° (2), and 80° (3)). The experimental data are represented by the points for the $\Delta(\omega)$ spectra. The measured phase hodographs in the inset in Fig. 8 correspond to the phase spectra 1, 2, and 3. It can be see that, as φ increases, the hodograph ring moves from left to right, and there are attained at some angles of incidence first the exciton Brewster effect and then the background effect.

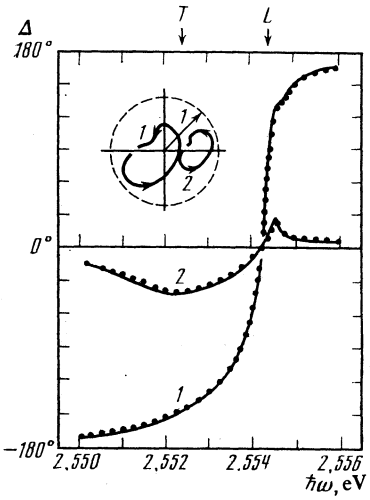

FIG. 7. Spectral dependence of the difference $\Delta = \Delta_p - \Delta_s$ between the phases of the reflectances r_p and r_s in the region of the $A_{n=1}$ exciton state of CdS crystals ($T = 2$ K) for angles of incidence $\varphi = 45°$ (the curve 1) and 80° (2). The points represent the experimental data; the curves, the theoretical results. The inset shows measured phase hodographs ($\rho = |r_p/r_s|$ versus Δ plots in polar coordinates) for angles of incidence $\varphi = 45°$ (1) and 80° (2). The crystal is oriented in such a way that the optical transition into the exciton state is allowed only for the p-polarized component of the light.

Since the qualitative picture of the behavior of the phase spectra and hodographs as functions of the angle of incidence is similar to the picture considered by us in the case of the ZnTe crystals (see Fig. 5), we shall not discuss Fig. 8 in

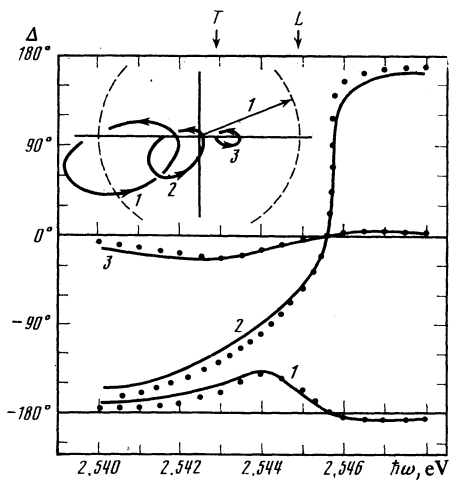

FIG. 8. Spectral dependence of the difference $\Delta = \Delta_p - \Delta_s$ between the phases of the reflectances r_p and r_s in the region of the $A_{n=1}$ exciton state of CdS crystals ($T = 77$ K) for angles of incidence $\varphi = 10°$ (the curve 1), 60° (2), and 80° (3). The points represent the experimental data; the curves, the theoretical results. The inset shows measured phase hodographs ($\rho = |r_p/r_s|$ versus Δ plots in polar coordinates)for angles of incidence $\varphi = 10°$ (1), 60° (2), and 80° (3). The crystal is oriented in such a way that the optical transition into the exciton state is allowed only for the p-polarized component of the light.

greater detail. Let us only note that in the case of the data shown in Fig. 8 the exciton and background Brewster angles are respectively equal to $\varphi_{BR}^{(p)} = 60°$ and $\varphi_0^{(p)} = 71.9°$.

§3. Comparison of the experimental data with theory; concluding remarks

The results, presented in the preceding section, of the experimental investigation of the oblique-incidence reflectance spectra of ZnTe, ZnP_2, and CdS crystals prove the existence of the exciton Brewster effect. In order to get some idea about the causes of the effect, we carried out a quantitative analysis of the experimental reflectance spectra R_p or R_s for definite angles of incidence ($\varphi = 45°$ for CdS and ZnTe, $\varphi = 10°$ for ZnP_2).

Particular attention was given to the quantitative agreement between the experimental and theoretical curves in the region of the reflectance minimum, since the minimum value of the reflectance is quite sensitive to the values of the layer thickness l and the damping constant Γ. In the case of the ZnTe, ZnP_2, and CdS crystals we were able to achieve at $T = 2$ K a good agreement between the theoretical and experimental curves within the limits of the entire reflectance contour, using a frequency-independent Γ value. But in the case of the CdS crystal at $T = 77$ K we have to take the value $\hbar\Gamma = 2.3$ meV in the region of the reflectance minimum and the value $\hbar\Gamma = 0.8$ meV in the region of the maximum.

The latter circumstance is apparently connected with the occurrence of a frequency-dependent exciton-phonon interaction in a sufficiently perfect crystal. At the same time, the nondependence on frequency of the parameter Γ in ZnTe is most likely due to the dominant contribution to the damping of the averaged exciton-impurity and exciton-defect interaction processes. If $\Gamma \ll \omega_{LT}$, then the reflectance contour is sensitive to the magnitude of the damping constant only in the region of the reflectance minimum. In such cases it is difficult to form an opinion about the frequency dependence of Γ on the basis of the reflectance spectra only.

The results of the analysis of the experimental reflectance spectra of the ZnTe, ZnP_2, and CdS crystals with the use of the theory described in Chap. I are presented in Table I and represented in Figs. 5–8 by the continuous curves for the phase spectra[2] $\Delta(\omega)$. In the table we give the values of the exciton-resonance parameters entering into the formula (1) of Chap. I, the dead-layer thickness l, and the computed—from the formulas (5)–(8)—and experimentally measured values of the angle of incidence φ_{BR} and frequency ω_{BR}.

Figures 5–8 clearly demonstrate the possibility of the practical use of the approximation (4) for the description of the exciton Brewster effect. Indeed the frequency $\omega'(\varphi)$ at which the coefficient r (the formula (2)) becomes real depends weakly on the angle of incidence φ. This manifests itself in the virtual constancy of the spectral location of the point where the phase Δ assumes the values $\pm\pi k$ ($k = 0, 1,...$).

In particular, the condition $r = 0$ is also realized at the frequency ω'; therefore, to estimate the value of the frequency ω_{BR}, we need only measure the spectrum $\Delta(\omega)$ at normal incidence, and find the point $\omega'(0°)$. The error $|\omega_{BR} - \omega'(0°)|/\omega_{LT}$ made when the frequency ω_{BR} is determined in this way is, in order of magnitude, equal to the ratio $\sin^2\varphi_{BR}/\varepsilon_0$. This fact manifests itself in Fig. 6, where the phase curves 1, 2, and 3 intersect the horizontal axes $\Delta = 0$, 180° at several differing frequencies.

Thus far, we have considered the situation in which the Brewster effect arises as the result of the variation of the angle of incidence of the light. At the same time, as follows from the theoretical curves shown in Figs. 2a and 3a, the effect can be attained by varying the damping constant Γ at a fixed angle of incidence. Since Γ depends on the crystal temperature, the exciton Brewster effect can be observed in experiment in the course of a gradual variation of the temperature.[2]

In Fig. 9 we schematically show the character of the variation at a fixed angle of incidence, of the phase spectra and the $\rho(\Delta)$ phase hodographs as functions of the quantity Γ for the p (a–c) and s (d–f) components of the reflected light.

For $\Gamma = \Gamma_{BR}$ the phase spectrum undergoes at the frequency ω_{BR} a jump equal either to $+\pi$ (the upward arrows in Figs. 9b and 9e or to $-\pi$ (the downward arrows in Figs. 9b and 9e). These jumps are physically indistinguishable, since the upper and lower phase curves in each of the figures (in the regions $\omega > \omega_{BR}$ in Fig. 9b and $\omega < \omega_{BR}$ in Fig. 9e) are

TABLE I

Crystal, light polarization	T, K	$\hbar\omega_0$, meV	$\hbar\omega_{LT}$, meV	M/m_0	ε_0	$\hbar\Gamma$, meV	l, Å	φ_{BR}, deg	$\hbar\omega_{BR}$, meV
ZnTe *p*-comp.	2	2380.9	0.54	2.3	8.7	0.8	132	theor. 59.9 exp. 62±2	theor. 2381.3 exp. 2381.4±0.1
ZnP_2 (orthorhom.) *s*-comp. $E \parallel C_{2z}$	2	1560.6	4.5	3.0	12.0	0.1	60	theor. 81.9 exp. 79±3	theor. 1565.4 exp. 1565.4±0.1
CdS *p*-comp. $E \perp C_6$	2	2552.4	2.0	0.9	10.0	0.075	70	No exciton Brewster effect	
CdS *p*-comp. $E \perp C_6$	77	2542.9	2.0	0.9	9.3	0.8 (ω_0) 2.3 (ω_L)	70	theor. 59.3 exp. 60±2	theor. 2545.9 exp. 2545.7±0.1

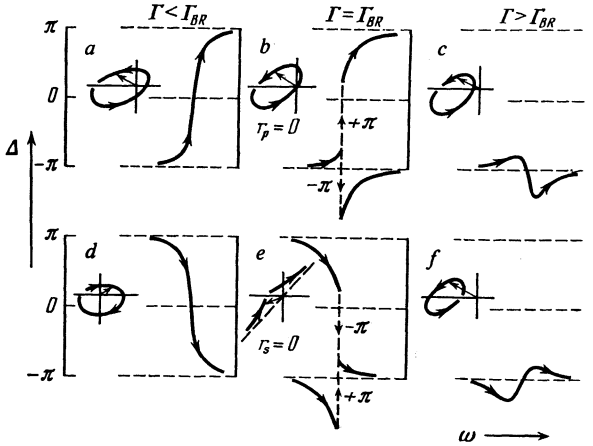

FIG. 9. The qualitative character of the variation, for a fixed angle of incidence, of the phase spectra $\Delta(\omega) = \Delta_p(\omega) - \Delta_s(\omega)$ and the phase hodographs $\rho(\Delta) = |r_p/r_s|$ as functions of the value of the damping constant Γ for the p (a–c) and s (d–f) components of the reflected light: a), d) $\Gamma < \Gamma_{BR}$; b), e) $\Gamma = \Gamma_{BR}$; c), f) $\Gamma > \Gamma_{BR}$, where Γ_{BR} is the value of Γ at which the reflectance vanishes ($r_p = 0$ (b), $r_s = 0$ (e)).

shifted relative to each other by 2π along the Δ scale. Therefore, when $\Gamma = \Gamma_{BR}$, the phase spectrum $\Delta(\omega)$ can be regarded as belonging simultaneously to the type shown in Figs. 9a and 9d and the type shown in Figs. 9c and 9f. A similar conclusion can be drawn on the basis of an examination of the corresponding hodographs in the upper left parts of Figs. 9b and 9e. As to the hodograph d, its shape corresponds to the requirement that $\rho \to \infty$ ($r_s \to 0$) as $\omega \to \omega_{BR}^{(s)}$. The $\rho(\Delta)$ curve in this case asymptotically approaches a straight line, whose slope determines the value of the phase at the points $\omega_{BR}^{(s)} \pm 0$.

The increase in the p component of the damping constant from a value $\Gamma < \Gamma_{BR}$ to a value $\Gamma > \Gamma_{BR}$ leads to a situation in which the hodograph ring shrinks to a discontinuity point whose location remains fixed. In the s component the discontinuity point also remains fixed, but the hodograph ring expands as $\Gamma \to \Gamma_{BR}$ ($\Gamma < \Gamma_{BR}$) and contracts upon further increase of Γ in the region $\Gamma > \Gamma_{BR}$. In this case the hodograph ring in the region $\Gamma > \Gamma_{BR}$ (e) is "inverted" with respect to the ring for $\Gamma < \Gamma_{BR}$ (d), which corresponds to the change in the direction of circulation about the hodograph at the point $\Gamma = \Gamma_{BR}$.

Thus, Fig. 9 allows us to offer the clear physical picture, referred to in Refs. 12 and 18, of the temperature dependence of the phase spectra.

Formulating the main result of the present paper, we note that the theoretical and experimental investigations, carried out by us, of the oblique-incidence exciton reflectance spectra prove the existence of the exact Brewster effect, which can be observed directly within the limits of the exciton reflectance band. The obtained agreement between the theoretical results and experiment gives grounds for believing that the dead-layer model sufficiently exactly reflects the characteristics of the behavior of the Wannier-Mott exciton in the surface region of the investigated crystals.

In conclusion, the authors express their gratitude to S. A. Permogorov for useful discussions.

[1)]We use the term Brewster effect to designate the vanishing of the reflectance for one of the polarization components.

[2)]Let us note that Moskovskiĭ *et al.*[23] have recently measured the phase spectra in the region of the exciton states of the ZnSe and CdSe crystals. The dependence of these spectra on the angle of incidence becomes apparent when considered within the framework of our approach.

1. M. Born and E. Wolf, Principles of Optics, Pergamon, Oxford, 1970 (Russ. Transl., Nauka, Moscow, 1970).
2. R. M. Azzam and N. M. Bashara, Elliptometry and Polarized Light, Elsevier-North Holland, New York, 1977 (Russ. Transl., Mir, Moscow, 1981).
3. H. Schopper, Optik **10**, 426 (1953).
4. J. J. Hopfield and D. G. Thomas, Phys. Rev. **132**, 563 (1963).
5. S. I. Pekar, Zh. Eksp. Teor. Fiz. **33**, 1022 (1957); **34**, 1176 (1958) [Sov. Phys. JETP **6**, 785 (1958); **7**, 851 (1958).
6. V. M. Agranovich and V. L. Ginzburg, Kristallooptika s uchetom prostranstvennoĭ dispersii i teorii éksitonov (Spatial Dispersion in crystal Optics and the Theory of Excitons), Nauka, Moscow, 1979 (Eng. Transl., Wiley, New York, 1967).
7. D. D. Sell, S. E. Stokowski, R. Dingle, and J. V. DiLorenzo, Phys.Rev. B **7**, 4568 (1973).
8. J. Lagous and K. Hummer, Phys. Status Solidi B **72**, 393 (1975).
9. F. Evangilisti, J. U. Fishbach, and A. Frova, Phys. Rev. B **9**, 1516 (1974).
10. I. Broser, M. Rosenzweig, R. Broser, M. Richard, and E. Birkicht, Phys. Status Solidi B **90**, 77 (1978).
11. E. L. Ivchenko and A. V. Sel'kin, Zh. Eksp. Teor. Fiz. **76**, 1837 (1979) [Sov. Phys. JETP **49**, 933 (1979)].
12. A. B. Pevtsov, A. S. Permogorov, Sh.R. Saĭfullaev, and A. V. Sel'kin, Fiz. Tverd. Tela (Leningrad) **22**, 2400 (1980) [Sov. Phys. Solid State **22**, 1396 (1980)].
13. B. Sermage, M. Voos, and C. Schwab, Phys. Rev. B **20**, 3245 (1979).
14. B. V. Novikov, G. Roppisher, and V. G. Talalaev, Fiz. Tverd. Tela (Leningrad) **21**, 823 (1979) [Sov. Phys. Solid State **21**, 481 (1979)].
15. T. M. Mashlyatina, D. S. Nedzvetskiĭ, and A. V. Sel'kin, Pis'ma Zh. Eksp. Teor. Fiz. **27**, 573 (1978) [JETP Lett. **27**, 539 (1978)].
16. A. B. Pevtsov and A. V. Sel'kin, Fiz. Tverd. Tela (Leningrad) **23**, 2814 (1981) [Sov. Phys. Solid State **23**, 1644 (1981)].
17. A. B. Pevtsov, S. A. Permogorov, A. V. Sel'kin, N. N. Syrbu, and A. G. Umanets, Fiz. Tekh. Poluprovodn. **16**, No. 8 (1982) [Sov. Phys. Semicond. **16**, (1982)].
18. A. V. Komarov, S. M. Ryabchenko, and M. I. Strashnikova, Zh. Eksp. Teor. Fiz. **74**, 251 (1978) [Sov. Phys. JETP **47**, 128 (1978)].
19. A. B. Pevtsov, S. A. Permogorov, and A. V. Sel'kin, Pis'ma Zh. Eksp. Teor. Fiz. **33**, 419 (1981) [JETP Lett. **33**, 402 (1981)].
20. I. Filinski and T. Skettrup, Solid State Commun. **11**, 1651 (1972).
21. L. E. Solov'ev and A. V. Babinskiĭ, Pis'ma Zh. Eksp. Teor. Fiz. **23**, 291 (1976) [JETP Lett. **23**, 263 (1976)].
22. M. V. Vol'kenshteĭn, Molekulyarnaya optika (Molecular Optics), Gostekhizdat, Moscow-Leningrad, 1951, p. 52.
23. S. B. Moskovskiĭ, L. E. Solov'ev, and M. O. Chaĭka, Fiz. Tverd, Tela (Leningrad) **23**, 3618 (1981) [Sov. Phys. Solid State **23**, 2102 (1981)].

Translated by A. K. Agyei